Varicella zoster virus–infected cerebrovascular cells produce a proinflammatory environment

OPEN

Dallas Jones, PhD
C. Preston Neff, PhD
Brent E. Palmer, PhD
Kurt Stenmark, MD
Maria A. Nagel, MD

Correspondence to
Dr. Nagel:
maria.nagel@ucdenver.edu

ABSTRACT

Objective: To test whether varicella zoster virus (VZV) infection of human brain vascular cells and of lung fibroblasts directly increases proinflammatory cytokine levels, consistent with VZV as a causative agent in intracerebral VZV vasculopathy and giant-cell arteritis (GCA).

Methods: Conditioned supernatant from mock- and VZV-infected human brain vascular adventitial fibroblasts (HBVAFs), human perineurial cells (HPNCs), human brain vascular smooth muscle cells (HBVSMCs), and human fetal lung fibroblasts (HFLs) were collected at 72 hours postinfection and analyzed for levels of 30 proinflammatory cytokines using the Meso Scale Discovery Multiplex ELISA platform.

Results: Compared with mock infection, VZV infection led to significantly increased levels of the following: interleukin-8 (IL-8) in all cell lines examined; IL-6 in HBVAFs, HPNCs, and HFLs, with no change in HBVSMCs; and vascular endothelial growth factor A in HBVAFs, HBVSMCs, and HFLs, with a significant decrease in HPNCs. Other cytokines, including IL-2, IL-4, IL-15, IL-16, TGF-b, Eotaxin-1, Eotaxin-3, IP-10, MCP-1, and granulocyte macrophage colony-stimulating factor, were also significantly altered upon VZV infection in a cell type–specific manner.

Conclusions: VZV infection of vascular cells can directly produce a proinflammatory environment that may potentially lead to prolonged arterial wall inflammation and vasculitis. The VZV-mediated increase in IL-8 and IL-6 is consistent with that seen in the CSF of patients with intracerebral VZV vasculopathy, and the VZV-mediated increase in IL-6 is consistent with the cytokine's elevated levels in temporal arteries and plasma of patients with GCA. ***Neurol Neuroimmunol Neuroinflamm* 2017;4:e382; doi: 10.1212/NXI.0000000000000382**

GLOSSARY

α-SMA = alpha–smooth muscle actin; **BBB** = blood-brain barrier; **FBS** = fetal bovine serum; **FACS** = fluorescence-activated cell sorting; **GCA** = giant-cell arteritis; **GM-CSF** = granulocyte macrophage colony-stimulating factor; **HBVAF** = human brain vascular adventitial fibroblast; **HBVSMC** = human brain vascular smooth muscle cell; **HFL** = human fetal lung fibroblast; **HPNC** = human perineurial cell; **IFNγ** = interferon gamma; **IL** = interleukin; **TARC** = thymus and activation-regulated chemokine; **TNF-α** = tumor necrosis factor alpha; **TNF-β** = tumor necrosis factor beta; **TGF-β** = transforming growth factor β; **VZV** = varicella zoster virus; **VEGF-A** = vascular endothelial growth factor A.

Varicella zoster virus (VZV) vasculopathy is due to productive virus infection of intracerebral arteries leading to stroke or aneurysm,[1,2] as supported by the presence of viral antigen, DNA, and herpesvirus particles in affected cerebral arteries of a patient with multiple infarcts[3,4] and by the presence of VZV antigen in a basilar artery aneurysm from a patient who died of cardiac arrest and subarachnoid hemorrhage 2 months after occipital distribution zoster.[5] Recent studies have expanded the spectrum of VZV vasculopathy to extracranial arteries. Indeed, VZV antigen was detected in 73/107 (70%) of temporal arteries from patients with giant-cell arteritis (GCA)[6]; in many of these arteries, VZV DNA and herpesvirus particles were also found.[7]

Analysis of cerebral and temporal arteries from patients with VZV vasculopathy has revealed loss of medial smooth muscle cells, a hyperplastic intima composed of cells expressing α-smooth

From the Department of Neurology (D.J., M.A.N.), Department of Medicine (C.P.N., B.E.P.), and Department of Pediatrics (K.S.), University of Colorado School of Medicine, Aurora.

Funding information and disclosures are provided at the end of the article. Go to Neurology.org/nn for full disclosure forms. The Article Processing Charge was funded by NIH AG032958.

muscle actin, and disruption of the internal elastic lamina.[8] A striking and consistent feature of VZV vasculopathy was arterial inflammation, consisting mostly of $CD4^+$ and $CD8^+$ T cells, as well as $CD68^+$ macrophages; neutrophils were abundant in the arterial adventitia during early but not late infection.[9] It is important that arterial inflammation was intimately associated with an overlying thickened intima, supporting the notion that inflammatory cells secrete soluble factors (e.g., cytokines and matrix metalloproteinases) that contribute to vascular injury, remodeling, and dysfunction.[9,10] Although the presence of VZV in conjunction with inflammation has been seen in both cerebral and temporal arteries in intracerebral VZV vasculopathy and GCA, respectively, VZV as the direct cause of arterial inflammation has not been demonstrated definitively. Thus, we tested whether VZV infection induces proinflammatory cytokines that result in arterial inflammation seen in VZV vasculopathy and GCA using 3 primary human brain vascular cell lines: (1) human brain vascular adventitial fibroblasts (HBVAFs), which are key regulators of vascular tone, function, and inflammation[11]; (2) human perineurial cells (HPNCs), the barrier cells surrounding adventitial nerve bundles that VZV must penetrate to infect adjacent vascular cells; and (3) human brain vascular smooth muscle cells (HBVSMCs), which are considered immunoprivileged[12] but may change the phenotype in response to VZV infection and migrate to form the thickened intima.[8] Human fetal lung fibroblasts (HFLs) served as control cells in this study.

METHODS

Virus and cells. Primary HBVAFs, HPNCs (Sciencell, Carlsbad, CA), and HFLs (ATCC, Manassas, VA) were seeded at 2,000 cells/cm^2 in a basal fibroblast medium with 2% fetal bovine serum (FBS), 1% fibroblast growth serum, and 1% 100× penicillin-streptomycin (Sciencell). HBVSMCs (Sciencell) were seeded at 2,000 cells/cm^2 in a basal smooth muscle cell medium with 2% FBS, 1% smooth muscle cell growth serum, and 1% 100× penicillin-streptomycin (Sciencell). After 24 hours, the medium was changed to basal fibroblast or basal smooth muscle cell medium with 0.1% FBS and 1% 100× penicillin-streptomycin that was replenished every 48–72 hours for 6–7 days to establish quiescence. At day 7, quiescent HBVAFs, HPNCs, HBVSMCs, and HFLs were cocultivated with VZV-infected (30–40 pfu/mL; Ellen strain)[13,14] or uninfected (mock-infected) HBVAFs, HPNCs, HBVSMCs, or HFLs, respectively. During the initial phase of cocultivation, a portion of cells in culture is infected; as infection progresses, virus spreads to adjacent cells. Depending on the amount of initial VZV-infected cells added and time, eventually all cells will be productively infected and die. Given the amount of virus in the inoculum used herein, at 72 hours of postinfection (hpi; height of cytopathic effect with 50–80% of cells infected), culture supernatants were collected and cells were harvested using sodium citrate[15] to optimize detection of cell surface proteins by flow cytometry.

Flow cytometry. Mock- and VZV-infected cells at 72 hpi were washed with fluorescence-activated cell sorting (FACS) buffer (phosphate-bufferedsaline containing 1% FBS) and stained with R-phycoerythrin–conjugated mouse anti-human anti-VZV-gE (Millipore, Billerica, MA) antibody using the SiteClick Antibody labeling kit (ThermoFisher, Waltham, MA) for 30 minutes at 4°C, washed with FACS buffer, and fixed with 1% paraformaldehyde. Isotype controls were used in all stainings. Cells were analyzed using a Canto-II or LSR-II flow cytometer (BD Immunocytometry Systems, San Jose, CA); >15,000 events were collected for all samples. Data were analyzed using Diva software (BD Biosciences) and FlowJo Software (Tree Star, Ashland, OR).

Multiplex electrochemiluminescence immunoassay. In the liquid phase from cell culture supernatants, levels of interleukin (IL)-1β, IL-1α, IL-2, IL-4, IL-5, IL-6, IL-7, IL-8, IL-10, IL-12p70, IL-12/23p40, IL-13, IL-15, IL-16, IL-17a, interferon gamma (IFNγ), tumor necrosis factor–alpha (TNF-α), tumor necrosis factor–beta (TNF-β), Eotaxin-1, Eotaxin-3, IFN-γ–induced protein 10 (IP-10), monocyte chemoattractant protein 1 (MCP1), MCP4, macrophage-derived chemokine (MDC), macrophage inflammatory protein 1–alpha (MIP-1α), MIP-1β, thymus and activation-regulated chemokine (TARC), granulocyte macrophage colony-stimulating factor (GM-CSF), and vascular endothelial growth factor–A (VEGF-A) were measured using the Meso Scale Discovery (MSD) human cytokine 30-Plex kit (Rockville, MD) according to the manufacturer's instructions. Levels of transforming growth factor-β1 (TGF-β1) were measured using the human TGF-β1 kit (MSD). For each cytokine, concentrations were calculated with reference to a standard curve derived using various concentrations of the standards assayed in the same manner as the cell culture supernatants. The lower limit of detection (LLOD) was calculated as the concentration of signal that was 2.5 SD above the zero calibrator. The upper limit of detection was calculated as the concentration of signal that was 2.5 SD below the upper plateau of the standard curve. All samples were analyzed in duplicate from triplicate experiments.

Statistical analysis. Statistical analysis was performed using GraphPad Prism (GraphPad, San Diego, CA). Statistical significance was determined using the Student *t* test.

RESULTS

Mock-infected HBVAFs secrete the highest basal level of cytokines compared with other mock-infected cells. Because adventitial fibroblasts in the outermost layer of arteries are key regulators of vascular tone, function, and inflammation,[11] basal levels of cytokines in mock-infected HBVAFs were compared with those in other mock-infected vascular cells (HPNCs and HBVSMCs) and in mock-infected HFLs commonly used to study VZV pathogenesis. As compared to mock-infected HPNCs, HBVSMCs, and HFLs (figure 1; red, blue, and green bars, respectively), mock-infected HBVAFs showed significantly higher levels of IL-2 ($p < 0.005$ for all); IL-6 ($p < 0.0005$, $p < 0.005$, and $p < 0.0005$,

Figure 1 **HBVAFs secrete the highest level of cytokines among vascular and lung cells**

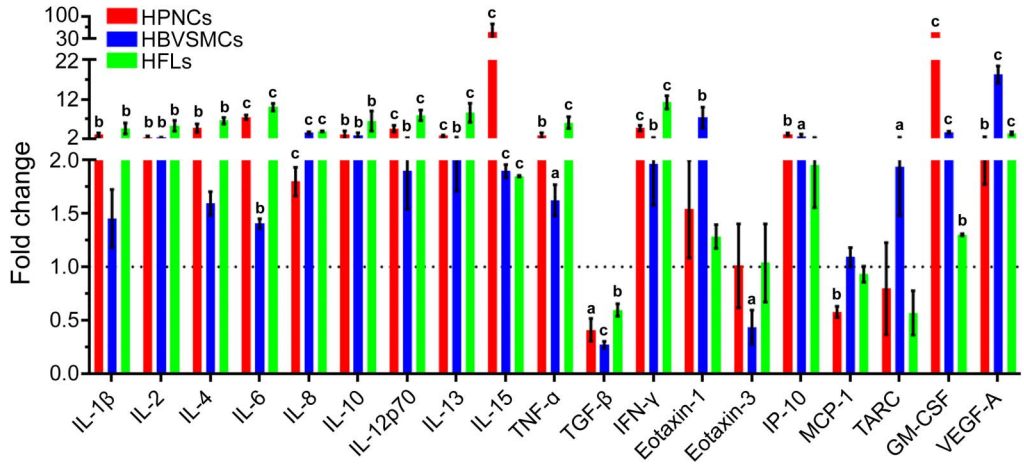

Cell culture supernatants from mock-infected HBVAFs, HPNCs, HBVSMCs, and HFLs were harvested at 72 hpi and analyzed for IL-1β, IL-1α, IL-2, IL-4, IL-5, IL-6, IL-7, IL-8, IL-10, IL-12p70, IL-12/23p40, IL-13, IL-15, IL-16, IL-17a, IFNγ, TNF-α, TNF-β, Eotaxin-1, Eotaxin-3, IP-10, MCP-1, MCP-4, MDC, MIP-1α, MIP-1β, TARC, GM-CSF, TGF-β, and VEGF-A levels. Only significant fold-change in HBVAFs cytokine levels compared with HPNCs (red), HBVSMCs (blue), or HFLs (green) were plotted. Bar graphs represent mean ± SEM fold-change in cytokine levels from triplicate experiments. (a) $p < 0.05$, (b) $p < 0.005$, and (c) $p < 0.0005$. GM-CSF = granulocyte macrophage colony-stimulating factor; HBVAF = human brain vascular adventitial fibroblast; HBVSMC = human brain vascular smooth muscle cell; HFL = human fetal lung fibroblast; HPNC = human perineurial cell; IL = interleukin; TNF-α = tumor necrosis factor alpha; TNF-β = tumor necrosis factor beta; TARC = thymus and activation-regulated chemokine; TGF-β = transforming growth factor β; VEGF-A = vascular endothelial growth factor A.

respectively); IL-8 ($p < 0.0005$ for all); IL-10 ($p < 0.005$ for all); IL-12p70 ($p < 0.0005$, $p < 0.005$, and $p < 0.0005$); IL-13 ($p < 0.0005$, $p < 0.005$, and $p < 0.0005$); IL-15 ($p < 0.0005$ for all); TNF-α ($p < 0.005$, $p < 0.05$, and $p < 0.0005$, respectively); IFN-γ ($p < 0.0005$, $p < 0.005$, and $p < 0.0005$, respectively); GM-CSF ($p < 0.0005$, $p < 0.0005$, and $p < 0.005$, respectively); and VEGF-A ($p < 0.005$, $p < 0.0005$, and $p < 0.0005$, respectively), whereas TGF-β levels were significantly decreased ($p < 0.05$, $p < 0.0005$, and $p < 0.005$, respectively). Unique differences in HBVAF cytokine levels compared with those of HPNCs included significant increases in IL-1β ($p < 0.005$), IL-4 ($p < 0.005$), and IP-10 ($p < 0.005$), but a significant decrease in MCP-1 ($p < 0.005$). Unique differences in HBVAF cytokine levels compared with HBVSMCs showed significant increases in Eotaxin-1 ($p < 0.005$), IP-10 ($p < 0.05$), and TARC ($p < 0.05$), but a significant decrease in Eotaxin-3 ($p < 0.05$), whereas the comparison with HFL cytokine levels revealed showed significant increases in IL-1β ($p < 0.005$) and IL-4 ($p < 0.005$).

Specific cytokines significantly altered during VZV infection of HBVAFs. To monitor VZV infection, mock- and VZV-infected HBVAFs were harvested at 72 hpi and analyzed for VZV gE expression using flow cytometry. VZV-infected HBVAFs were >80% VZV gE+. Compared with the supernatant from mock-infected HBVAFs, the supernatant from VZV-infected HBVAFs had significantly increased levels of IL-8 ($p = 0.02$), IL-6 ($p = 0.03$), VEGF-A ($p = 0.001$), TGF-β ($p = 0.04$), and IL-16 ($p = 0.01$), along with significantly decreased levels of Eotaxin-1 ($p = 0.002$), MCP-1 ($p = 0.003$), IP-10 ($p = 0.02$), and GM-CSF ($p = 0.03$) (table and figure 2). Levels of the remaining 21 analytes were either undetectable or not significantly changed.

Specific cytokines significantly altered during VZV infection of HPNCs. VZV-infected HPNCs at 72 hpi were >85% VZV gE+. Compared with the supernatant from mock-infected HPNCs, the supernatant from VZV-infected HPNCs had significantly increased levels of IL-8 ($p = 0.05$), IL-6 ($p = 0.006$), IL-2 ($p = 0.03$), and GM-CSF ($p = 0.02$), along with significantly decreased levels of VEGF-A ($p = 0.003$) (table and figure 3). Levels of the remaining 25 analytes were either undetectable or not significantly changed.

Specific cytokines significantly altered during VZV infection of HBVSMCs. VZV-infected HBVSMCs at 72 hpi were >50% VZV gE+. Compared with the supernatant from mock-infected HBVSMCs, the supernatant from VZV-infected HBVSMCs had significantly increased levels of IL-8 ($p = 0.002$) and VEGF-A ($p = 0.0004$), along with significantly decreased levels of IL-15 ($p = 0.006$), Eotaxin-3 ($p = 0.004$), IP-10 ($p = 0.02$), and MCP-1 ($p = 0.02$) (table and figure 4). Levels of the remaining 24

Table Meso Scale Discovery analyte levels from mock- and VZV-infected HBVAFs, HPNCs, HBVSMCs, and HFLs

	HBVAFs, Mock/VZV	HPNCs, Mock/VZV	HBVSMCs, Mock/VZV	HFLs, Mock/VZV	LLOD-ULOD
IL-1β	0.372 ± 0.100	0.131 ± 0.078	0.268 ± 0.110	0.083 ± 0.067	0.140-575.0
	0.221 ± 0.123	0.150 ± 0.099	0.211 ± 0.094	0.175 ± 0.092	
IL-1α	Undetectable	Undetectable	Undetectable	Undetectable	0.0989-405.0
	Undetectable	Undetectable	0.101 ± 0.084	Undetectable	
IL-2	1.09 ± 0.183	0.458 ± 0.044[a]	0.492 ± 0.123	0.221 ± 0.068	0.381-1,560.0
	1.18 ± 0.175	0.624 ± 0.083[a]	0.703 ± 0.202	0.477 ± 0.237	
IL-4	0.250 ± 0.059	0.055 ± 0.016	0.159 ± 0.04	0.038 ± 0.015[a]	0.0583-239.0
	0.323 ± 0.045	0.084 ± 0.017	0.198 ± 0.048	0.063 ± 0.016[a]	
IL-5	Undetectable	Undetectable	Undetectable	Undetectable	0.223-912.0
	Undetectable	Undetectable	Undetectable	Undetectable	
IL-6	437.7 ± 32.85[a]	59.44 ± 2.4[a]	315.2 ± 23.0	44.8 ± 4.9[a]	0.182-745.0
	630.5 ± 45.72[a]	74.7 ± 5.0[a]	275.3 ± 22.5	74.6 ± 10.7[a]	
IL-7	Undetectable	Undetectable	Undetectable	Undetectable	0.205-838.0
	Undetectable	Undetectable	Undetectable	Undetectable	
IL-8	546.9 ± 38.5[a]	305.4 ± 16.0[a]	158.8 ± 11.9[a]	140.8 ± 8.0[a]	0.163-666.0
	695.1 ± 56.6[a]	345.3 ± 18.9[a]	234.8 ± 9.2[a]	223.1 ± 26.3[a]	
IL-10	0.366 ± 0.061	0.136 ± 0.059	0.135 ± 0.038	0.078 ± 0.053	0.0891-365.0
	0.369 ± 0.109	0.168 ± 0.028	0.207 ± 0.075	0.109 ± 0.041	
IL-12p70	1.313 ± 0.096	0.303 ± 0.083	0.736 ± 0.20	0.152 ± 0.095	0.119-489.0
	1.414 ± 0.235	0.411 ± 0.038	0.741 ± 0.234	0.188 ± 0.093	
IL-12/23p40	Undetectable	Undetectable	Undetectable	Undetectable	0.786-3,220.0
	Undetectable	Undetectable	Undetectable	Undetectable	
IL-13	3.488 ± 0.184	1.287 ± 0.224	1.798 ± 0.476	0.511 ± 0.331	0.123-505.0
	4.089 ± 0.454	2.143 ± 0.212	2.271 ± 0.693	1.074 ± 0.380	
IL-15	1.483 ± 0.071	0.154 ± 0.273	0.783 ± 0.013[b]	0.802 ± 0.035[a]	0.190-779.0
	1.482 ± 0.099	0.322 ± 0.395	0.504 ± 0.044[b]	1.135 ± 0.157[a]	
IL-16	Undetectable[a]	Undetectable	Undetectable	Undetectable	0.618-2,530.0
	1.177 ± 0.824[a]	Undetectable	Undetectable	Undetectable	
IL-17a	Undetectable	Undetectable	Undetectable	Undetectable	1.47-6,010.0
	Undetectable	Undetectable	Undetectable	Undetectable	
TNF-α	0.537 ± 0.06	0.212 ± 0.079	0.337 ± 0.09	0.10 ± 0.045	0.0901-369.0
	0.601 ± 0.11	0.309 ± 0.058	0.442 ± 0.12	0.233 ± 0.099	
TNF-β	Undetectable	Undetectable	Undetectable	Undetectable	0.154-632.0
	Undetectable	Undetectable	Undetectable	Undetectable	
TGF-β	132.3 ± 28.9[a]	352.5 ± 92.9	498.8 ± 42.4	222.7 ± 22.3[a]	17.0-100,000.0
	256.7 ± 66.5[a]	337.8 ± 36.1	532.4 ± 92.8	786.2 ± 193.1[a]	
IFN-γ	3.049 ± 0.341	0.677 ± 0.40	1.64 ± 0.41	Undetectable	0.396-1,620.0
	3.221 ± 0.887	1.005 ± 0.248	1.871 ± 0.90	Undetectable	
Eotaxin-1	13.56 ± 2.81[b]	9.98 ± 4.13	2.72 ± 2.70	10.51 ± 7.91	0.366-1,500.0
	1.174 ± 1.758[b]	8.82 ± 2.82	Undetectable	7.26 ± 2.0	
Eotaxin-3	3.257 ± 2.144	3.917 ± 1.953	8.063 ± 2.154[b]	2.413 ± 2.224	1.21-4,970.0
	1.877 ± 1.412	6.687 ± 3.303	3.62 ± 1.869[b]	3.369 ± 1.806	
IP-10	2.418 ± 0.546[b]	0.771 ± 0.177	1.007 ± 0.434[b]	1.312 ± 0.693	0.586-2,400.0
	0.425 ± 0.103[b]	1.031 ± 0.181	0.308 ± 0.073[b]	0.794 ± 0.249	
MCP-1	142.3 ± 11.05[b]	445.2 ± 96.32	130.8 ± 25.9[b]	180.4 ± 69.17	0.109-448.0

Continued

Table Continued

	HBVAFs, Mock/VZV	HPNCs, Mock/VZV	HBVSMCs, Mock/VZV	HFLs, Mock/VZV	LLOD-ULOD
	58.11 ± 18.40[b]	356.6 ± 90.12	71.19 ± 13.59[b]	210 ± 71.95	
MCP-4	16.79 ± 5.81	29.26 ± 10.0	16.49 ± 5.81	20.65 ± 7.95	0.147-602.0
	19.64 ± 3.45	29.30 ± 3.58	12.49 ± 7.25	24.17 ± 6.60	
MDC	Undetectable	4.085 ± 2.20	Undetectable	Undetectable	2.59-10,600.0
	Undetectable	2.985 ± 0.66	Undetectable	Undetectable	
MIP-1α	Undetectable	8.345 ± 3.69	Undetectable	Undetectable	0.230-942.0
	Undetectable	4.834 ± 3.16	Undetectable	Undetectable	
MIP-1β	Undetectable	Undetectable	Undetectable	Undetectable	0.247-1,010.0
	Undetectable	Undetectable	Undetectable	Undetectable	
TARC	3.068 ± 0.973	6.005 ± 4.93	1.649 ± 0.311	6.369 ± 5.774	0.366-1,500.0
	3.689 ± 3.66	3.831 ± 1.783	3.494 ± 2.456	2.68 ± 1.03	
GM-CSF	14.54 ± 0.46[b]	0.06 ± 0.10[a]	4.001 ± 0.378	11.17 ± 4.17	0.243-996.0
	12.17 ± 1.04[b]	2.52 ± 1.16[a]	3.953 ± 0.190	10.19 ± 2.43	
VEGF-A	310.9 ± 16.3[a]	152.7 ± 52.5[b]	17.7 ± 4.59[a]	94.5 ± 26.3[a]	0.249-1,020.0
	523.4 ± 23.6[a]	9.58 ± 2.9[b]	127.4 ± 3.6[a]	366.9 ± 108.7[a]	

Abbreviations: GM-CSF = granulocyte macrophage colony-stimulating factor; HBVAF = human brain vascular adventitial fibroblast; HBVSMC = human brain vascular smooth muscle cell; HFL = human fetal lung fibroblast; HPNC = human perineurial cell; IL = interleukin; LLOD = lower limit of detection; ULOD = upper limit of detection; TARC = thymus and activation-regulated chemokine; TGF-β = transforming growth factor β; TNF-α = tumor necrosis factor alpha; TNF-β = tumor necrosis factor beta; VEGF-A = vascular endothelial growth factor A; VZV = varicella zoster virus.
[a] Significantly increased cytokine levels in VZV-infected vs mock-infected cells.
[b] Significantly decreased cytokine levels in VZV-infected vs mock-infected cells.

analytes were either undetectable or not significantly changed.

Specific cytokines significantly induced during VZV infection of HFLs. As a positive control for cytokine secretion during VZV infection, we analyzed cytokine levels in mock- and VZV-infected HFLs. VZV-infected HFLs at 72 hpi were >80% VZV gE+. Compared with mock-infected HFLs, VZV-infected HFLs had significantly increased levels of IL-8 ($p = 0.02$), IL-6 ($p = 0.02$), VEGF-A ($p = 0.01$), TGF-β ($p = 0.01$), IL-15 ($p = 0.04$), and IL-4 ($p = 0.05$) (table and figure 5). Levels of the remaining 24 analytes were either undetectable or not significantly changed.

DISCUSSION Herein, we show that VZV infection of primary HPNCs, brain vascular adventitial fibroblasts and vascular smooth muscle cells, as well as lung fibroblasts significantly upregulates multiple proinflammatory cytokines, consistent with the notion that VZV infection of vascular cells can initiate infiltration of inflammatory cells, vasculopathy, and ultimately stroke or GCA. Thus, the association of VZV and inflammation is unlikely to reflect preexisting inflammation triggering VZV reactivation; rather, VZV directly contributes to vasculitis.

Several proinflammatory cytokines important in persistent inflammation and vascular remodeling, i.e., IL-8, IL-6, GM-CSF, VEGF-A, TGF-β, IL-15, and IL-16, were altered in response to VZV infection and warrant further discussion. For example, IL-8 (CXCL8), which promotes neutrophil migration to the site of infection and activation through degranulation,[16] was the only cytokine/chemokine elevated in all 4 cell lines studied. This finding is consistent with a significant increase of IL-8 levels in the CSF of patients with VZV vasculopathy compared with CSF from both patients with MS and healthy controls.[17] Moreover, robust IL-8 induction explains the neutrophil infiltration seen in VZV-infected temporal arteries[9] and the predominance of neutrophils in CSF of patients with VZV vasculopathy.[18] Finally, on discontinuation of corticosteroids in patients with GCA, serum IL-8 increases and neutrophils are activated,[19] strongly suggesting that the underlying cause of GCA, i.e., VZV, is still present to trigger arterial inflammation.

Levels of IL-6, an acute-phase proinflammatory cytokine that promotes monocyte differentiation into macrophages,[20] were increased in VZV-infected in HPNCs, HBVAFs, and HFLs, as also seen in the CSF of patients with VZV vasculopathy.[17] Indeed, macrophages represent a dominant immune infiltrate in VZV-infected arteries from patients with intracerebral VZV vasculopathy, as well as GCA.[7,9] In HBVSMCs, the lack of a VZV-induced increase in IL-6, as well as decreases in IL-15, Eotaxin-3, IP-10, and MCP-1, adds another contributing factor to the

Figure 2 **Specific cytokines significantly altered during VZV infection in HBVAFs**

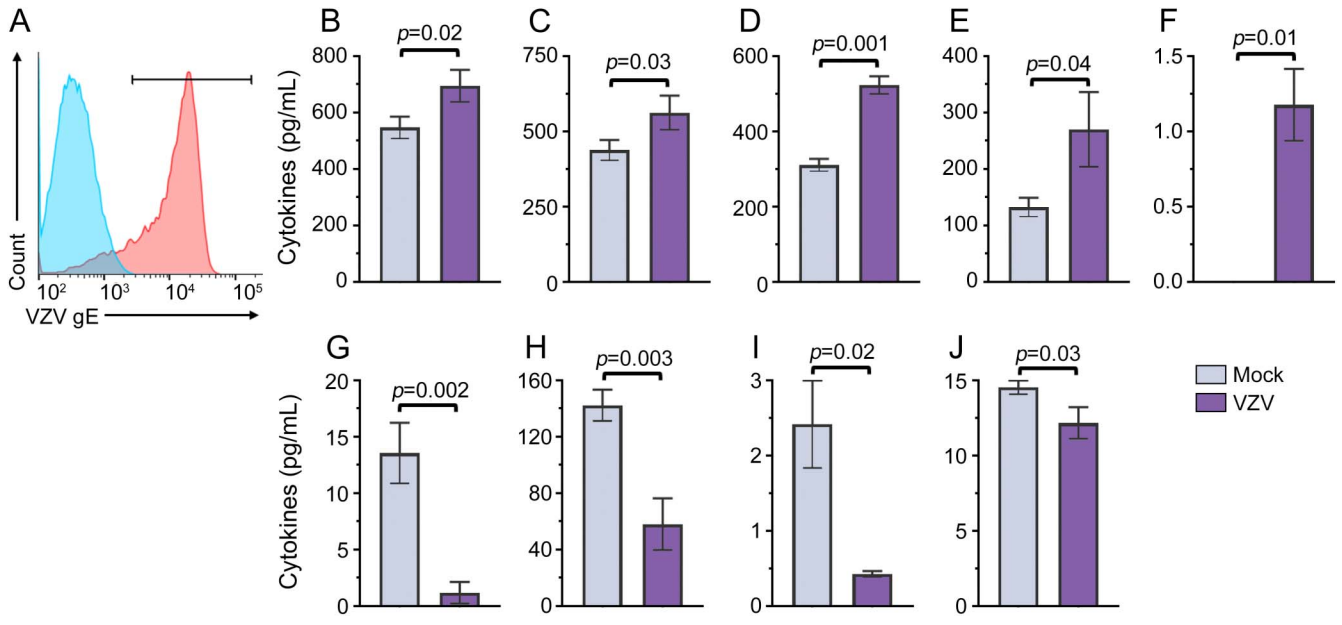

Cells and cell culture supernatants were harvested at 72 hpi from mock- or VZV-infected HBVAFs. (A) Flow cytometry analyses of VZV gE expression in mock- (blue) and VZV-infected (red) HBVAFs at 72 hpi showed that >80% of cells were VZV gE+. Cells were gated using isotype controls. Compared with cell culture supernatants from mock-infected cells, supernatants from VZV-infected HBVAFs had significantly higher levels of IL-8 (B; $p = 0.02$), IL-6 (C; $p = 0.03$), VEGF-A (D; $p = 0.001$), TGF-β (E; $p = 0.04$), and IL-16 (F; $p = 0.01$). Compared with cell culture supernatants from mock-infected cells, supernatants from VZV-infected HBVAFs had significantly lower levels of Eotaxin-1 (G; $p = 0.002$), MCP-1 (H; $p = 0.003$), IP-10 (I; $p = 0.02$), and GM-CSF (J; $p = 0.03$). All cytokine values are given in picograms per milliliter. Bar graphs represent mean ± SD cytokine levels from 3 independent experiments. GM-CSF = granulocyte macrophage colony-stimulating factor; HBVAF = human brain vascular adventitial fibroblast; IL = interleukin; TGF-β = transforming growth factor β; VEGF-A = vascular endothelial growth factor A; VZV = varicella zoster virus.

immunoprivileged status of VSMCs.[12] Previous studies have shown that smooth muscle cells intrinsically lack essential costimulators, particularly OX40L, that activate memory T cells.[21] Our finding that the proinflammatory response to virus infection is also reduced in smooth muscle cells may contribute to the lack of medial inflammation during early VZV infection.[6] The lack of IL-6 induction in VZV-infected HBVSMCs might also represent a protective host mechanism because IL-6 induces smooth muscle cell apoptosis.[22]

Two other cytokines involved in macrophage maturation and activation were differentially regulated in VZV-infected HBVAFs and HPNCs. GM-CSF

Figure 3 **Specific cytokines significantly altered during VZV infection in HPNCs**

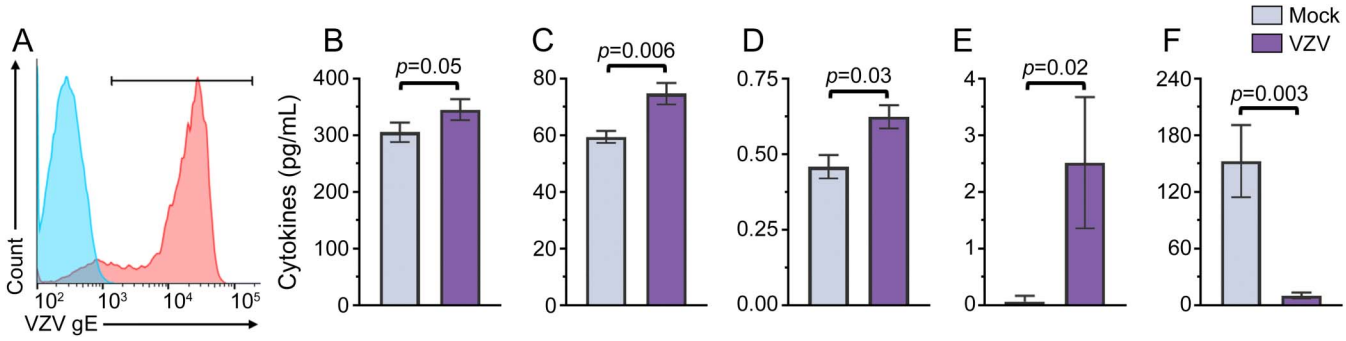

Cells and cell culture supernatants were harvested at 72 hpi from mock- or VZV-infected HPNCs. (A) Flow cytometry analyses of VZV gE expression in mock- (blue) and VZV-infected (red) HPNCs at 72 hpi showed that >85% of cells were VZV gE+. Cells were gated using isotype controls. Compared with cell culture supernatants from mock-infected cells, supernatants from VZV-infected HPNCs had significantly higher levels of IL-8 (B; $p = 0.05$), IL-6 (C; $p = 0.006$), IL-2 (D; $p = 0.03$), and GM-CSF (E; $p = 0.02$). Compared with cell culture supernatants from mock-infected cells, supernatants from VZV-infected HPNCs had significantly lower levels of VEGF-A (F; $p = 0.003$). All cytokine values are given in picograms per milliliter. Bar graphs represent mean ± SD cytokine levels from 3 independent experiments. GM-CSF = granulocyte macrophage colony-stimulating factor; HPNC = human perineurial cell; IL = interleukin; VEGF-A = vascular endothelial growth factor A; VZV = varicella zoster virus.

Figure 4 Cytokines significantly altered during VZV infection in HBVSMCs

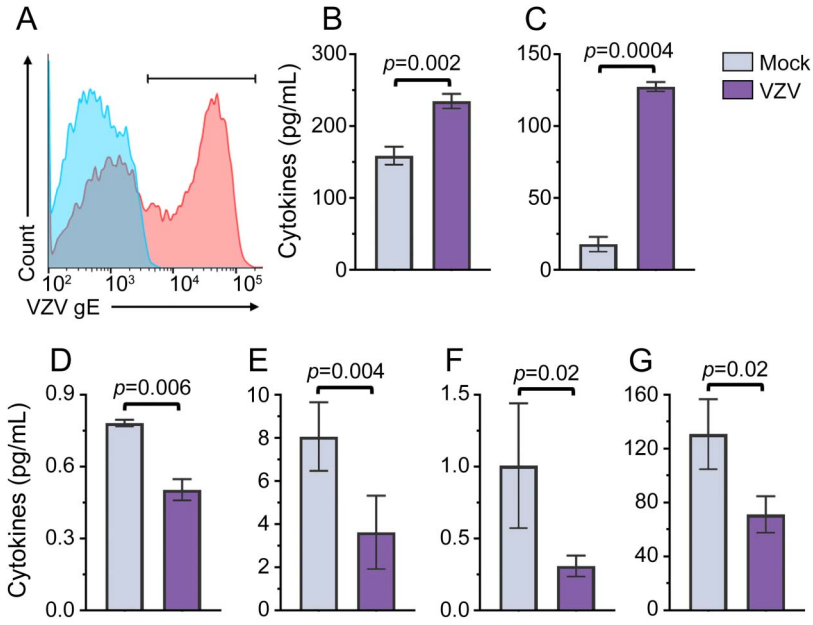

Cells and cell culture supernatants were harvested at 72 hpi from mock- or VZV-infected HBVSMCs. (A) Flow cytometry analyses of VZV gE expression in mock- (blue) and VZV-infected (red) HBVSMCs at 72 hpi showed that >50% of cells were VZV gE+. Cells were gated using isotype controls. Compared with cell culture supernatants from mock-infected cells, supernatants from VZV-infected HBVSMCs had significantly higher levels of IL-8 (B; $p = 0.002$) and VEGF-A (C; $p = 0.0004$). Compared with cell culture supernatants from mock-infected cells, supernatants from VZV-infected HBVSMCs had significantly lower levels of IL-15 (D; $p = 0.006$), Eotaxin-3 (E; $p = 0.004$), IP-10 (F; $p = 0.02$), and MCP-1 (G; $p = 0.02$). All cytokine values are given in picograms per milliliter. Bar graphs represent mean ± SD cytokine levels from 3 independent experiments. HBVSMC = human brain vascular smooth muscle cell; IL = interleukin; VEGF-A = vascular endothelial growth factor A; VZV = varicella zoster virus.

levels were increased in VZV-infected HPNCs, promoting macrophage maturation in conjunction with IL-6, whereas infected HBVAFs had decreased GM-CSF, as well as decreased MCP-1, which would diminish macrophage maturation/activation during the later stages of infection compared with HPNCs. Perineurial cells are the first cells infected by VZV during reactivation, and their enhanced levels of GM-CSF and IL-6 during infection could be the initial stimulus to activate and differentiate monocytes into macrophages and retain them in the infected artery. As virus spreads to the adventitia without proper clearance, VZV-infected HBVAFs secrete less GM-CSF, potentially preventing macrophage activation and explaining the presence of macrophages in arteries up to 10 months after diagnosis of VZV vasculopathy.

The most significantly altered secretory protein observed in all 4 cell lines analyzed was VEGF-A, with levels significantly increased in VZV-infected HBVAFs, HBVSMCs, and HFLs, but significantly decreased in infected HPNCs. VEGF-A is of particular importance during VZV vasculopathy as it promotes angiogenesis, along with being a chemotactic protein for macrophages and neutrophils.[23] The role of VEGF-A in stroke is contextual and can be both beneficial and problematic.[23] The benefits of VEGF-A include neuronal protection, vasodilation, and angiogenesis; however, high levels of VEGF-A can increase blood-brain barrier (BBB) leakage to produce poststroke brain edema and severe intracranial hypertension.[24,25] Patients with high basal levels of VEGF-A have a greater risk of stroke.[26–28] In addition, analyses in murine models of stroke have shown that prompt administration of VEGF-A increased stroke severity, whereas prompt VEGF-A blockade reduced infarct size and swelling.[24,25] Thus, the VZV-mediated induction of VEGF-A in HBVAFs and HBVSMCs would worsen the severity of VZV vasculopathy because these infected cells in the artery would be a continual source of VEGF-A acting to disrupt the BBB, enhance intracranial hypertension, and promote macrophage/neutrophil infiltration. Note that simian varicella virus infection induced VEGF-A, along with IL-8 and IL-6, during acute infection in rhesus macaques,[29] further supporting the VZV-mediated induction of VEGF-A reported herein. Although diminished VEGF-A secretion by VZV-infected HPNCs in the artery could initially prevent these adverse effects of VEGF-A, virus is not cleared from this cellular layer during reactivation and can spread to the adventitia and smooth muscle cell layer. Diminished VEGF-A secretion by VZV-infected HPNCs might reflect the delay in neuronal/arterial protection required for viral spread and VZV vasculopathy onset.

Both VZV-infected HBVAFs and HFLs showed significantly increased secretion of TGF-β, a pleotropic cytokine that can induce migration and proliferation.[30] This increase in TGF-β mediated by VZV could enhance the migration of adventitial fibroblasts in the infected artery, promoting the vascular remodeling that is a hallmark of stroke/vasculitis. TGF-β is also an immunosuppressive cytokine that would diminish viral clearance in the infected artery and possibly explain our recent finding of VZV-mediated downregulation of major histocompatibility complex-I in uninfected bystander cells.[31]

Along with TGF-β, IL-16, a cytokine that activates $CD4^+$ T cells and can be secreted by TGF-β–stimulated fibroblasts,[32] was also significantly elevated in VZV-infected HBVAFs, consistent with the infiltrate of $CD4^+$ T cells observed in both early and late VZV vasculopathy. Significant elevations in IL-2 secretion seen in VZV-infected HPNCs would also aid in T-cell activation. Of interest, VZV has a tropism for $CD4^+$ T cells, and the induction of IL-2 and IL-16 in the infected arteries could aid in the viral tropism for these cells. Both VZV-infected HBVAFs and HBVSMCs also secreted significantly less IP-10,

Figure 5 Cytokines significantly induced during VZV infection in HFLs

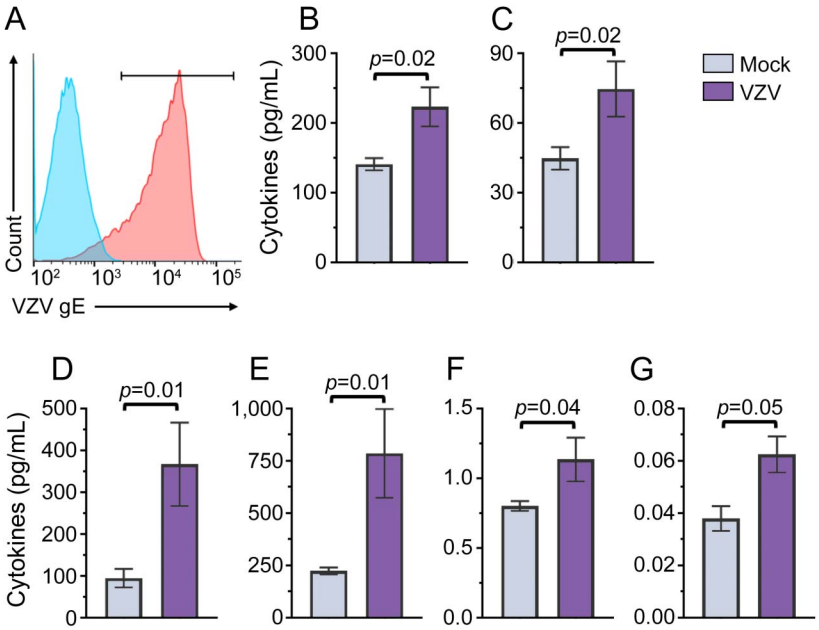

Cells and culture supernatants were harvested at 72 hpi from mock- or VZV-infected HFLs. (A) Flow cytometry analyses of VZV gE expression in mock- (blue) and VZV-infected (red) HFLs at 72 hpi showed that >80% of cells were VZV gE+. Cells were gated using isotype controls. Compared with cell culture supernatants from mock-infected cells, supernatants from VZV-infected HFLs had significantly higher levels of IL-8 (B; $p = 0.02$), IL-6 (C; $p = 0.02$), VEGF-A (D; $p = 0.01$), TGF-β (E; $p = 0.01$), IL-15 (F; $p = 0.04$), and IL-4 (G; $p = 0.05$). All cytokine values are given in pg/ml. Bar graphs represent mean ± SD cytokine levels from 3 independent experiments. HFL = human fetal lung fibroblast; IL = interleukin; TGF-β = transforming growth factor β; VEGF-A = vascular endothelial growth factor A; VZV = varicella zoster virus.

which could inhibit viral clearance in the infected artery because IP-10 acts as a chemoattractant for activated T cells and is required for host defense against virus-induced neurologic disorders.[33] The VZV-mediated targeting of this pathway to promote viral spread and persistent inflammation during VZV vasculopathy is supported by analysis of IP-10 murine knockout models, which revealed a dramatic reduction in viral clearance and enhanced inflammation during infection of the eye with herpes simplex-1, another member of the alpha-herpesviridae subfamily, compared with wild-type mice.[34]

IL-15 is a proinflammatory cytokine that activates natural killer cells and enhances memory $CD8^+$ T-cell responses.[35] Based on the functional properties of this cytokine, the VZV-mediated induction of IL-15 in HFLs could enhance viral clearance in the lung during primary infection. VZV-infected HBVSMCs had significantly reduced levels of secreted IL-15, which has been shown to inhibit smooth muscle cell proliferation.[36] Furthermore, blockade of IL-15 during arterial injury increased intimal thickening in mice,[37] a finding particularly relevant in VZV vasculopathy because a thickened intima and smooth muscle cell migration and differentiation into a myofibroblast phenotype are hallmarks of this disease, along with pulmonary hypertension and stroke in general.[11]

Overall, our comprehensive analysis of the cytokines secreted by multiple cells in the artery and by lung fibroblasts after VZV infection shows that the virus significantly upregulates and downregulates several cytokines in various combinations distinct for each cell type. Most notable in VZV-infected vascular cells is the detection of elevated IL-8 and IL-6, which promote neutrophil and macrophage migration/activation in the infected artery, as well as the detection of elevated VEGF-A, which promotes BBB permeability and immune infiltration. Of interest, IL-6 is the major cytokine involved in GCA pathogenesis,[38–40] whereas IL-8 and VEGF-A have been found to play a major role in disease progression as well.[39] Together with a previous report that VZV-infected arteries downregulate PD-L1 to promote persistent inflammation,[31] these data demonstrate that VZV infection is sufficient to promote a proinflammatory environment within 72 hours, which may potentially lead to a persistent vasculitis, and support VZV as the causative agent in intracerebral VZV vasculopathy and GCA.

AUTHOR CONTRIBUTIONS

Dr. Jones: drafted and revised the manuscript for content, and collected, analyzed, and interpreted the data. Dr. Neff: assisted with sample analysis and drafted and revised the manuscript. Dr. Palmer: assisted with sample analysis and drafted and revised the manuscript. Dr. Stenmark: assisted with sample analysis and drafted and revised the manuscript. Dr. Nagel: drafted and revised the manuscript for content; designed and supervised the study; and collected, analyzed, and interpreted the data.

ACKNOWLEDGMENT

The authors thank Marina Hoffman for editorial review and Cathy Allen for word processing and formatting.

STUDY FUNDING

This work was supported in part by the NIH grants NS094758 and AG032958 to M.A.N.

DISCLOSURE

D. Jones and C. Preson Neff report no disclosures. B.E. Palmer received research support from NIH/NIDDK and NHLBI. K. Stenmark served on the scientific advisory board for Pfizer, Entelligence/Actelion, and ContraFect; served on the editorial board for *American Journal of Respiratory and Critical Care Medicine*, *American Journal of Physiology—Lung Cellular and Molecular Physiology*, *Circulation Research*, *Pulmonary Circulation*, *American Journal of Respiratory Cell and Molecular Biology*; consulted for Novartis and ContraFect; and received research support from NIH, Axis, and Department of Defense. M.A. Nagel received research support from NIH. Go to Neurology.org/nn for full disclosure forms.

Received January 9, 2017. Accepted in final form May 16, 2017.

REFERENCES

1. Nagel MA, Cohrs RJ, Mahalingam R, et al. The varicella zoster virus vasculopathies: clinical, CSF, imaging, and virologic features. Neurology 2008;70:853–860.
2. Liberman AL, Nagel MA, Hurley MC, Caprio FZ, Bernstein RA, Gilden D. Rapid development of 9 cerebral

aneurysms in varicella-zoster virus vasculopathy. Neurology 2014;82:2139–2141.
3. Case records of the Massachusetts General Hospital. Weekly clinicopathological exercises. Case 5-1995. A 73-year-old man with focal brain lesions and peripheral-nerve disease. N Engl J Med 1995;332:452–459.
4. Gilden DH, Kleinschmidt-DeMasters BK, Wellish M, Hedley-Whyte ET, Rentier B, Mahalingam R. Varicella zoster virus, a cause of waxing and waning vasculitis: the New England Journal of Medicine case 5-1995 revisited. Neurology 1996;47:1441–1446.
5. Fukumoto S, Kinjo M, Hokamura K, Tanaka K. Subarachnoid hemorrhage and granulomatous angiitis of the basilar artery: demonstration of the varicella-zoster-virus in the basilar artery lesions. Stroke 1986;17:1024–1028.
6. Gilden D, White T, Khmeleva N, Boyer PJ, Nagel MA. VZV in biopsy-positive and -negative giant cell arteritis: analysis of 100+ temporal arteries. Neurol Neuroimmunol Neuroinflamm 2016;3:e216. doi: 10.1212/NXI.0000000000000216.
7. Gilden D, White T, Khmeleva N, et al. Prevalence and distribution of VZV in temporal arteries of patients with giant cell arteritis. Neurology 2015;84:1948–1955.
8. Nagel MA, Traktinskiy I, Azarkh Y, et al. Varicella zoster virus vasculopathy: analysis of virus-infected arteries. Neurology 2011;77:364–370.
9. Nagel MA, Traktinskiy I, Stenmark KR, Frid MG, Choe A, Gilden D. Varicella-zoster virus vasculopathy: immune characteristics of virus-infected arteries. Neurology 2013;80:62–68.
10. Sprague AH, Khalil RA. Inflammatory cytokines in vascular dysfunction and vascular disease. Biochem Pharmacol 2009;78:539–552.
11. Stenmark KR, Yeager ME, El Kasmi KC, et al. The adventitia: essential regulator of vascular wall structure and function. Annu Rev Physiol 2013;75:23–47.
12. Dal Canto AJ, Swanson PE, O'Guin AK, Speck SH, Virgin HW. IFN-gamma action in the media of the great elastic arteries, a novel immunoprivileged site. J Clin Invest 2001;107:R15–R22.
13. Grose C, Brunel PA. Varicella-zoster virus: isolation and propagation in human melanoma cells at 36 and 32 degrees C. Infect Immun 1979;19:199–203.
14. Cohrs RJ, Wischer J, Essman C, Gilden DH. Characterization of varicella-zoster virus gene 21 and 29 proteins in infected cells. J Virol 2002;76:7228–7238.
15. Zhang B, Shan H, Li D, et al. Different methods of detaching adherent cells significantly affect the detection of TRAIL receptors. Tumori 2012;98:800–803.
16. Baggiolini M, Walz A, Kunkel SL. Neutrophil-activating peptide-1/interleukin 8, a novel cytokine that activates neutrophils. J Clin Invest 1989;84:1045–1049.
17. Jones D, Alvarez E, Selva S, Gilden D, Nagel MA. Proinflammatory cytokines and matrix metalloproteinases in CSF of patients with VZV vasculopathy. Neurol Neuroimmunol Neuroinflamm 2016;3:e246. doi: 10.1212/NXI.0000000000000246.
18. Haug A, Mahalingam R, Cohrs RJ, Schmid DS, Corboy JR, Gilden D. Recurrent polymorphonuclear pleocytosis with increased red blood cells caused by varicella zoster virus infection of the central nervous system: case reports and review of the literature. J Neurol Sci 2010;292:85–88.
19. Nadkami S, Dalli J, Hollywood J, Mason JC, Dasgupta B, Perretti M. Investigational analysis reveals a potential role for neutrophils in giant-cell arteritis disease progress. Circ Res 2014;114:242–248.
20. Chomarat P, Banchereau J, Davoust J, Palucka AK. IL-6 switches the differentiation of monocytes from dendritic cells to macrophages. Nat Immunol 2000;1:510–514.
21. Zhang P, Manes TD, Pober JS, Tellides G. Human vascular smooth muscle cells lack essential costimulatory molecules to activate allogeneic memory T cells. Arterioscler Thromb Vasc Biol 2010;30:1795–1801.
22. Yu H, Clarke MC, Figg N, Littlewood TD, Bennett MR. Smooth muscle cell apoptosis promotes vessel remodeling and repair via activation of cell migration, proliferation, and collagen synthesis. Arterioscler Thromb Vasc Biol 2011;31:2402–2409.
23. Lange C, Storkebaum E, de Almodovar CR, Dewerchin M, Carmeliet P. Vascular endothelial growth factor: a neurovascular target in neurological diseases. Nat Rev Neurol 2016;12:439–454.
24. Zhang ZG, Zhang L, Jiang Q, et al. VEGF enhances angiogenesis and promotes blood-brain barrier leakage in the ischemic brain. J Clin Invest 2000;106:829–838.
25. van Bruggen N, Thibodeaux H, Palmer JT, et al. VEGF antagonism reduces edema formation and tissue damage after ischemia/reperfusion injury in the mouse brain. J Clin Invest 1999;104:1613–1620.
26. Mellergard P, Sjogren F, Hillman J. Release of VEGF and FGF in the extracellular space following severe subarachnoidal haemorrhage or traumatic head injury in humans. Br J Neurosurg 2010;24:261–267.
27. Slevin M, Krupinski J, Slowik A, Kumar P, Szczudlik A, Gaffney J. Serial measurement of vascular endothelial growth factor and transforming growth factor-beta1 in serum of patients with acute ischemic stroke. Stroke 2000;31:1863–1870.
28. Pikula A, Beiser AS, Chen TC, et al. Serum brain-derived neurotrophic factor and vascular endothelial growth factor levels are associated with risk of stroke and vascular brain injury: Framingham Study. Stroke 2013;44:2768–2775.
29. Arnold N, Girke T, Sureshchandra S, Nguyen C, Rais M, Messaoudi I. Genomic and functional analysis of the host response to acute simian varicella infection in the lung. Sci Rep 2016;6:34164.
30. Xu J, Lamouille S, Derynck R. TGF-beta-induced epithelial to mesenchymal transition. Cell Res 2009;19:156–172.
31. Jones D, Blackmon A, Neff CP, et al. Varicella-zoster virus downregulates programmed death ligand 1 and major histocompatibility complex class I in human brain vascular adventitial fibroblasts, perineurial cells, and lung fibroblasts. J Virol 2016;90:10527–10534.
32. Franz JK, Kolb SA, Hummel KM, et al. Interleukin-16, produced by synovial fibroblasts, mediates chemoattraction for CD4+ T lymphocytes in rheumatoid arthritis. Eur J Immunol 1998;28:2661–2671.
33. Liu MT, Chen BP, Oertel P, et al. The T cell chemoattractant IFN-inducible protein 10 is essential in host defense against viral-induced neurologic disease. J Immunol 2000;165:2327–2330.
34. Shen FH, Wang SW, Yeh TM, Tung YY, Hsu SM, Chen SH. Absence of CXCL10 aggravates herpes stromal keratitis with reduced primary neutrophil influx in mice. J Virol 2013;87:8502–8510.
35. Schluns KS, Williams K, Ma A, Zheng XX, Lefrancois L. Cutting edge: requirement for IL-15 in the generation of

primary and memory antigen-specific CD8 T cells. J Immunol 2002;168:4827–4831.
36. Iwasaki S, Minamisawa S, Yokoyama U, et al. Interleukin-15 inhibits smooth muscle cell proliferation and hyaluronan production in rat ductus arteriosus. Pediatr Res 2007;62:392–398.
37. Cercek M, Matsumoto M, Li H, et al. Autocrine role of vascular IL-15 in intimal thickening. Biochem Biophys Res Commun 2006;339:618–623.
38. Martinez-Taboada VM, Alvarez L, RuizSoto M, Marin-Vidalled MJ, Lopez-Hoyos M. Giant cell arteritis and polymyalgia rheumatica: role of cytokines in the pathogenesis and implications for treatment. Cytokine 2008;44:207–220.
39. Ly KH, Regent A, Tamby MC, Mouthon L. Pathogenesis of giant cell arteritis: more than just an inflammatory condition? Autoimmun Rev 2010;9:635–645.
40. Guillevin L, Regent A. Treating giant-cell arteritis: is IL-6 the cytokine to target? Lancet 2016;387:1882–1883.

Neurology®
Neuroimmunology
& Neuroinflammation

Varicella zoster virus–infected cerebrovascular cells produce a proinflammatory environment

Dallas Jones, C. Preston Neff, Brent E. Palmer, et al.

Neurol Neuroimmunol Neuroinflamm 2017;4;
DOI 10.1212/NXI.0000000000000382